British Journal of Pharmacology (2004) 141, 457–467
www.nature.com/bjp

Characterization of an anandamide degradation system in prostate epithelial PC-3 cells: synthesis of new transporter inhibitors as tools for this study

[1,6]Lidia Ruiz-Llorente, [2,6]Silvia Ortega-Gutiérrez, [2]Alma Viso, [1]María G. Sánchez, [1]Ana M. Sánchez, [3]Carlos Fernández, [4]José A. Ramos, [5]Cecilia Hillard, [1,3]Miguel A. Lasunción, [2]María L. López-Rodríguez & *,[1]Inés Díaz-Laviada

[1]Departamento de Bioquímica y Biología Molecular, Facultad de Medicina, Universidad de Alcalá, Alcalá de Henares, 28871 Madrid, Spain; [2]Departamento de Química Orgánica, Facultad de Químicas, Universidad Complutense, 28040 Madrid, Spain; [3]Servicio de Bioquímica-Investigación, Hospital Ramón y Cajal, 28034 Madrid, Spain; [4]Departamento de Bioquímica y Biología Molecular III, Facultad de Medicina, Universidad Complutense, 28040 Madrid, Spain and [5]Department of Pharmacology, Medical College of Wisconsin, 8701 Watertown Plank Rd, Milwaukee, WI 53226-0509, U.S.A.

1 The response of anandamide is terminated by a carrier-mediated transport followed by degradation catalyzed by the cloned enzyme fatty acid amidohydrolase (FAAH). In this study, we provide biochemical data showing an anandamide uptake process and the expression of FAAH in human prostate.

2 Anandamide was accumulated in PC-3 cells by a saturable and temperature-dependent process. Kinetic studies of anandamide uptake, determined in the presence of cannabinoid and vanilloid antagonists, revealed apparent parameters of $K_M = 4.7 \pm 0.2\,\mu M$ and $V_{max} = 3.3 \pm 0.3$ pmol min^{-1} (10^6 cells)$^{-1}$.

3 The accumulation of anandamide was moderately inhibited by previously characterized anandamide transporter inhibitors (AM404, UCM707 and VDM11) but was unaffected by inhibitors of other lipid transport systems (phloretin or verapamil) and moderately affected by the FAAH inhibitor methyl arachidonyl fluorophosphonate.

4 The presence of FAAH in human prostate epithelial PC-3 cells was confirmed by analyzing its expression by Western blot and measuring FAAH activity.

5 To further study the structural requirements of the putative carrier, we synthesized a series of structurally different compounds **1**–**8** and evaluated their capacity as uptake inhibitors. They showed different inhibitory capacity in PC-3 cells, with (9*Z*,12*Z*)-*N*-(fur-3-ylmethyl)octadeca-9,12-dienamide (**4**, **UCM119**) being the most efficacious, with maximal inhibition and IC_{50} values of 49% and $11.3 \pm 0.5\,\mu M$, respectively.

6 In conclusion, PC-3 cells possess a complete inactivation system for anandamide formed by an uptake process and the enzyme FAAH. These results suggest a possible physiological function of anandamide in the prostate, reinforcing the role of endocannabinoid system as a neuroendocrine modulator.

British Journal of Pharmacology (2004) **141,** 457–467. doi:10.1038/sj.bjp.0705628

Keywords: Anandamide degradation; anandamide uptake inhibitors; prostate PC-3 cells; fatty acid amidohydrolase; endogenous cannabinoid system

Abbreviations: AA, arachidonic acid; AM404, *N*-(4-hydroxyphenyl)-arachidonamide; ANA, *N*-arachidonoylethanolamine, anandamide; CB_1, cannabinoid receptor of type 1; CB_2, cannabinoid receptor of type 2; DCC, dicyclohexylcarbodiimide; DMAP, 4-(dimethylamino)pyridine; EDTA, ethylenediaminetetraacetic acid; EGTA, ethylene glycol-bis (*β*-amino ethyl ether) tetraacetic acid; FAAH, fatty acid amidohydrolase; MAFP, methyl arachidonyl fluorophosphonate; PBS, phosphate-buffered saline; PC-3, prostate carcinoma cells; PMSF, phenylmethanesulfonyl fluoride; RBL-2H3, rat basophilic leukemia cells; SAR, structure–activity relationship; s.e., standard error; SR141716A, *N*-(piperidin-1-yl)-5-(4-chlorophenyl)-1-(2,4-dichlorophenyl)-4-methyl-1*H*-pyrazole-3-carboxamide hydrochloride; SR144528, *N*-[(1*S*)-*endo*-1,3,3-trimethyl-bicyclo[2.2.1]heptan-2-yl]-5-(4-chloro-3-methylphenyl)-1-(4-methylbenzyl)-pyrazole-3-carboxamide; TCA, trichloroacetic acid; TLC, thin-layer chromatography; UCM119, (9*Z*,12*Z*)-*N*-(fur-3-ylmethyl)octadeca-9,12-dienamide; UCM707, *N*-(fur-3-ylmethyl)arachidonamide; VDM11, *N*-(4-hydroxy-2-methylphenyl) arachidonamide; VR_1, vanilloid receptor of type 1; K_M, Michaelis constant; V_{max}, maximum accumulation rate

Introduction

Although research on the molecular bases of the physiological effects of marijuana use was slowed for many years due to the

*Author for correspondence; E-mail: ines.diazlaviada@uah.es
[6]Contributed equally to this study
Advance online publication: 12 January 2004

lack of specific technology, much progress has been achieved in cannabinoid research in the last decade. Many of the physiological and pharmacological actions of plant-derived cannabinoids are mimicked by endogenous substances named endocannabinoids. The first characterized endocannabinoid was *N*-arachidonoylethanolamine (anandamide, ANA) (Devane *et al*., 1992), which has been found in several mammalian tissues and reproductive fluids (Schuel *et al*., 2002). Endocannabinoids are now presented as new neuromodulators acting through specific cannabinoid receptors (Di Marzo *et al*., 1998; Wilson & Nicoll, 2002). To date, two cannabinoid receptors that belong to the seven-transmembrane G protein-coupled receptors superfamily, CB_1 and CB_2 (cannabinoid receptor of type 1 and 2, respectively), have been cloned in humans (Sugiura & Waku, 2002). CB_1 receptors are expressed in several brain regions (reviewed in Ameri, 1999) and also in some peripheral tissues and cell lines, whereas CB_2 receptors are mostly confined to immune tissues (Klein *et al*., 2001). Additionally, anandamide can also activate the binding site for capsaicin, the pungent principle in hot pepper, named vanilloid VR_1 (vanilloid receptor of type 1) receptor (Smart *et al*., 2000). The termination of the action of anandamide is achieved through its uptake by cells and subsequent enzymatic degradation, catalyzed by the specific enzyme fatty acid amidohydrolase (FAAH) (Giuffrida *et al*., 2001; Deutsch *et al*., 2002; Cravatt & Lichtman, 2003). The uptake of anandamide by intact neurons is mediated by a high-affinity, rapid, saturable, selective and temperature-dependent carrier that is not affected by fatty acids, arachidonate metabolites, neurotransmitters or biogenic amines (firstly described by Di Marzo *et al*. (1994) and reviewed in Giuffrida *et al*. (2001), Hillard & Jarrahian (2000) and Fowler & Jacobsson (2002)). Mechanisms of endocannabinoid inactivation may also exist in peripheral tissues, and they have been detected in macrophages and rat basophilic leukemia cells (RBL-2H3) (Bisogno *et al*., 1997), platelets (Maccarrone *et al*., 2001), human endothelial cells (Maccarrone *et al*., 2000a) and mouse Sertoli cells (Maccarrone *et al*., 2003). Because of this rapid deactivation process, it could be deemed likely that cannabinoid receptors and the putative cannabinoid transporter are close together in the same or neighboring cells. It has been previously described that human prostate epithelial cells (Ruiz *et al*., 1999; Melck *et al*., 2000; Velasco *et al*., 2001) and human prostate gland (Ruiz-Llorente *et al*., 2003) express cannabinoid receptors suggesting a functional role of cannabinoids in the prostate gland. In fact, morphological and functional alterations of human prostate gland have been observed in chronic exposure of laboratory animals to (−)-Δ^9-tetrahydrocannabinol (THC) (Harclerode, 1984) and in male rats exposed *in utero* to THC (Ahluwalia *et al*., 1985). It has also been described that cannabinol and THC inhibit specific binding of dihydrotestosterone to the androgen receptor in the prostate gland (Purohit *et al*., 1980). Moreover, there is evidence that suggests that the endocannabinoid system has an important role in the regulation of endocrine functions, and recent results support the consideration of endocannabinoids as neuroendocrine modulators (Wenger *et al*., 2001; Maccarrone *et al*., 2002, 2003; Wenger & Moldrich, 2002). Accordingly, it is of importance to determine the mechanisms of degradation of endocannabinoids, in particular anandamide as the most representative one, in target glands of the hypothalamic-pituitary-gonadal axis. It has been recently shown that cannabinoids regulate the proliferation of prostate cells (Melck *et al*., 2000; Mimeault *et al*., 2003; Sánchez *et al*., 2003), suggesting that cannabinoids not only modulate hormone levels but have a direct action on prostate development. In this study we focus on the degradation system of anandamide in prostate, an issue that has remained unapproached to date. We show that anandamide is accumulated in prostate carcinome cells (PC-3) cells by a saturable and temperature-dependent process. The accumulation of anandamide is inhibited by previously characterized anandamide transporter inhibitors such as *N*-(4-hydroxyphenyl)arachidonamide (AM404) and *N*-(fur-3-ylmethyl)arachidonamide (UCM707), which block transport with moderate efficacy, and *N*-(4-hydroxy-2-methylphenyl) arachidonamide (VDM11), which caused a 49% of inhibition. New synthesized inhibitors (**1**–**8**) were also tested for their efficacy to inhibit anandamide transporter. Among them, (9*Z*,12*Z*)-*N*-(fur-3-ylmethyl)octadeca-9,12-dienamide (compound **4**, UCM119) deserves special attention as it was as potent as VDM11 in PC-3 cells (UCM119 maximal inhibition = 49%; $IC_{50} = 11.3\,\mu M$). Additionally, we provide evidence about the expression of FAAH by human prostate gland and prostate epithelial cell lines. All these data suggest the existence of a complete anandamide inactivation system in PC-3 cells constituted by an uptake process together with the expression of the FAAH. This study reinforces the notion that the endocannabinoid system plays a physiological function in the prostate.

Methods

Reagents

Arachidonyl-[5,6,8,9,11,12,14,15-^{3}H]-ethanolamide ([^{3}H]-anandamide, [^{3}H]-ANA, 200 Ci mmol^{-1}) was obtained from American Radiolabeled Chemicals, Inc. (St Louis, MO, U.S.A.). Unlabeled anandamide was from Sigma (St Louis, MO, U.S.A.). AM404, VDM11, methyl arachidonyl fluorophosphonate (MAFP) and capsazepine were purchased from Tocris (Avonmouth, Bristol, U.K.). Phloretin and (±)-verapamil hydrochloride were from Sigma (St Louis, MO, U.S.A.). Cannabinoid receptor antagonists SR141716A (*N*-(piperidin-1-yl)-5-(4-chlorophenyl)-1-(2,4-dichlorophenyl)-4-methyl-1*H*-pyrazole-3-carboxamide hydrochloride) and SR144528 (*N*-[(1*S*)-*endo*-1,3,3-trimethyl-bicyclo[2.2.1]heptan-2-yl]-5-(4-chloro-3-methylphenyl)-1-(4-methylbenzyl)-pyrazole-3-carboxamide) were a kind gift from Sanofi Recherche (Montpellier, France). Other agents were from Sigma (St Louis, MO, U.S.A.). FAAH antiserum was generously donated by C.J. Hillard (Medical College of Wisconsin, U.S.A.). Peroxidase-conjugated goat anti-rabbit immunoglobulin (Ig) G was from Santa Cruz Biotechnology (Santa Cruz, CA, U.S.A.).

Chemistry

Starting materials used were high-grade commercial products from Aldrich, Acros, Fluka, Merck or Panreac. Arachidonic (AA) (90% of purity), palmitic, oleic, linoleic and linolenic acids were purchased from Sigma. All reagents were used as supplied except methylene chloride, which was distilled over CaH_2 before use. Fur-3-ylmethylamine, (5*Z*,8*Z*,11*Z*,14*Z*)-

N-(fur-3-ylmethyl)icosa-5,8,11,14-tetraenamide (**1**, UCM707), *S*-(fur-2-ylmethyl) (5*Z*,8*Z*,11*Z*,14*Z*)-icosa-5,8,11,14-tetraenethioate (**6**), (±) (5*Z*,8*Z*,11*Z*,14*Z*)-*N*-[(1-methyl-2-thien-3-yl)ethyl]icosa-5,8,11,14-tetraenamide (**7**) and 2-(1*H*-indol-3-yl)ethyl (5*Z*,8*Z*,11*Z*,14*Z*)-icosa-5,8,11,14-tetraenoate (**8**) were synthesized as previously described (López-Rodríguez *et al*., 2001a, b; 2003; Fowler *et al*., 2003).

Infrared (IR) spectra were determined on a Perkin-Elmer 781 or Shimadzu-8300 infrared spectrophotometer. ^{1}H- and ^{13}C-NMR spectra were recorded on a Varian VXR-300S, Bruker Avance 300-AM or Bruker 200-AC instrument at room temperature (RT). Chemical shifts (δ) are expressed in parts per million relative to internal tetramethylsilane; coupling constants (J) are in hertz. Satisfactory elemental analyses were obtained for all the newly synthesized analogs and are within $\pm$0.4% of the theoretical values. Thin-layer chromatography (TLC) was run on Merck silica gel 60 F-254 plates. For normal pressure chromatography, Merck silica gel type 60 (size 70-230) was used.

*General procedure for the synthesis of derivatives **2–5***

A solution of dicyclohexylcarbodiimide (DCC, 1 equivalent) and 4-(dimethylamino)pyridine (DMAP, 0.068 equivalents) in dry methylene chloride (3 ml mmol^{-1} DCC) was added dropwise to a stirred solution of one equivalent (0.33 mmol) of the corresponding fatty acid in dry methylene chloride (1 ml mmol^{-1}) and fur-3-ylmethylamine (1.5 equivalents) in dry methylene chloride (1 ml mmol^{-1}) at -20°C in a salt-ice-bath and under argon. The mixture was stirred for 5 min at this temperature and then the cooling bath was removed and stirred at RT (3–6 h) until no further evolution was observed by TLC (chloroform : methanol, 95 : 5). The dicyclohexylurea was filtered off, the filtrate evaporated under reduced pressure and the residue obtained was taken up in methylene chloride (20 ml mmol^{-1} of fatty acid). This resulting organic phase was washed with a cooled 0.5 M hydrochloric acid solution and brine, and the organic extracts dried over Na_2SO_4 or $MgSO_4$. Then, the solvent was evaporated under reduced pressure and the product purified by column chromatography on silica gel using the appropriate eluent.

*(9Z)-**N**-(fur-3-ylmethyl)octadec-9-enamide (**2**)* Yield = 55%; R_f = 0.18 (hexane : chloroform, 2 : 8); IR ($CDCl_3$, cm^{-1}): 3296, 2928, 2854, 1657, 1514, 1466, 1385, 1161, 1070, 1022; ^{1}H-NMR (200 MHz, $CDCl_3$-δ): 0.87 (t, 3H, J = 6.6 Hz), 1.26–1.29 (m, 20H), 1.58–1.66 (m, 2H), 1.95–2.01 (m, 4H), 2.17 (t, 2H, J = 7.8 Hz), 4.20 (d, 2H, J = 5.5 Hz), 5.30–5.36 (m, 2H), 5.74 (br s, 1H), 6.34–6.35 (m, 1H), 7.34–7.37 (m, 2H); ^{13}C-NMR (50 MHz, $CDCl_3$-δ): 14.1, 22.6, 25.7, 27.1, 27.2, 29.1, 29.2 (2C), 29.3 (2C), 29.5, 29.7 (2C), 31.9, 34.3, 36.7, 110.4, 122.5, 129.8, 130.1, 140.2, 143.5, 173.1.

*(9Z)-**N**-(fur-3-ylmethyl)hexadec-9-enamide (**3**)* Yield = 65%; R_f = 0.17 (hexane : chloroform, 2 : 8); IR (CH_2Cl_2, cm^{-1}): 3296, 2926, 2854, 1643, 1543, 1466, 1159, 1022, 876; ^{1}H-NMR (200 MHz, $CDCl_3$-δ): 0.88 (t, 3H, J = 6.8 Hz), 1.28–1.29 (m, 16H), 1.59–1.66 (m, 2H), 1.98–2.01 (m, 4H), 2.17 (t, 2H, J = 6.8 Hz), 4.21 (d, 2H, J = 5.5 Hz), 5.25–5.42 (m, 2H), 5.64 (br s, 1H), 6.34–6.36 (m, 1H), 7.35–7.38 (m, 2H); ^{13}C-NMR (50 MHz, $CDCl_3$-δ): 14.1, 22.6, 25.7, 27.1, 27.2, 29.0, 29.1, 29.2 (2C), 29.7 (2C), 31.8, 34.4, 36.7, 110.2, 122.4, 129.7, 130.0, 140.1, 143.4, 173.0.

*(9Z,12Z)-**N**-(fur-3-ylmethyl)octadeca-9,12-dienamide (**4**, UCM119)* Yield = 65%; R_f = 0.22 (chloroform); IR ($CDCl_3$, cm^{-1}): 3294, 3009, 2928, 2854, 2245, 1643, 1545, 1504, 1466, 1433, 1387, 1271, 1161, 1022, 874; ^{1}H-NMR (200 MHz, $CDCl_3$-δ): 0.82 (t, 3H, J = 6.9 Hz), 1.19–1.35 (m, 14H), 1.53–1.60 (m, 2H), 1.93–1.99 (m, 4H), 2.11 (t, 2H, J = 7.9 Hz), 2.70 (t, 2H, J = 5.6 Hz), 4.21 (d, 2H, J = 5.5 Hz), 5.19–5.38 (m, 4H), 5.63 (br s, 1H), 6.28–6.30 (m, 1H), 7.30–7.31 (m, 2H); ^{13}C-NMR (50 MHz, $CDCl_3$-δ): 13.9, 22.4, 25.4, 25.5, 27.0 (2C), 28.9 (2C), 29.1, 29.2, 29.4, 31.3, 34.2, 36.5, 110.1, 122.1, 127.7, 127.8, 129.8, 130.0, 139.9, 143.3, 172.9.

*(9Z,12Z,15Z)-**N**-(fur-3-ylmethyl)octadeca-9,12,15-trienamide (**5**)* Yield = 60%; R_f = 0.14 (chloroform); IR (CH_2Cl_2, cm^{-1}): 3296, 3011, 2926, 2852, 1634, 1543, 1159, 1022, 876; ^{1}H-NMR (200 MHz, $CDCl_3$-δ): 0.96 (t, 3H, J = 7.6 Hz), 1.23–1.34 (m, 8H), 1.59–1.69 (m, 2H), 2.00–2.21 (m, 6H), 2.80 (t, 4H, J = 5.6 Hz), 4.27 (d, 2H, J = 5.6 Hz), 5.23–5.46 (m, 6H), 5.69 (br s, 1H), 6.34–6.35 (m, 1H), 7.34–7.35 (m, 2H); ^{13}C-NMR (50 MHz, $CDCl_3$-δ): 14.3, 20.6, 25.5, 25.6, 25.7, 27.2, 29.1, 29.2 (2C), 29.6, 34.4, 36.8, 110.3, 122.5, 127.1, 127.7, 128.2, 128.3, 130.2, 132.0, 140.2, 143.5, 173.0.

Cell cultures

Human prostate PC-3 cells were purchased from American Type Culture Collection (Rockville, MD, U.S.A.). They were routinely grown in RPMI 1640 medium supplemented with 10% fetal calf serum. For experiments, cells were seeded at 22,000 cells cm^{-2} in six-well dishes and grown for 2 days. At 24 h before the experiment, the serum-containing medium was removed and cells were transferred to a chemically defined medium consisting of RPMI 1640 supplemented with 5 μg ml^{-1} insulin, 5 μg ml^{-1} transferrin and 5 ng ml^{-1} sodium selenite.

The number of cells was determined in parallel using a Neubauer chamber.

Determination of cellular [^{3}H]-anandamide uptake

Incorporation of ANA into PC-3 cells was determined by incubating cells with a mixture of [^{3}H]-ANA (see reagents for [^{3}H]ANA specification) and ANA in a 1/500 relationship to different final concentrations and during different intervals according to the experiments. The cellular uptake was terminated by placing the plates on ice, rapid aspiration of the medium, washing four times with 0.5 ml of ice-cold phosphate-buffered saline (PBS), pH 7.4, containing 1% fatty acid free bovine serum albumin (BSA) and subsequent protein precipitation with 10% trichloroacetic acid (TCA). The plates were kept on ice for additional 15 min and 0.5 ml of a 1 M sodium hydroxide solution was added. Then, the plates were incubated for 1 h at RT and assayed for tritium content by liquid scintillation.

For inhibition assays, cells were preincubated at 37°C for 15 min in the presence or absence of several concentrations of the tested carrier-mediated anandamide transport inhibitors and incubated with 100 nM ANA for 5 min.

Nonspecific ANA incorporation was determined by parallel incubations carried out at 4°C. These values were subtracted

from the total amount of ANA incorporated. To determinate the non-specific binding to plastic plates, six well plates without cells at 37°C were also run in parallel for some of the experiments and the results obtained turned out to be essentially comparable to the values obtained at 4°C in the presence of cells.

To study whether ANA bound to CB_1, CB_2 or VR_1 could influence total ANA accumulation, incubations were carried out as previously described preincubating cells for 15 min with 50 μM SR141716A, 50 μM SR144528 and 50 μM capsazepine.

To study the influence of FAAH or other lipid transporters in ANA uptake, another set of studies were carried out in the presence of 100 μM of the FAAH inhibitors MAFP and phenylmethanesulfonyl fluoride (PMSF) or other lipid uptake inhibitors such as phloretin or verapamil.

Kinetic studies of the ANA incorporation were performed following the same procedure at different incubation times, and using [^{3}H]-ANA diluted with cold ANA to yield total concentrations ranging from 10 nM to 25 μM ANA.

Data analyses

The Michaelis constant (K_M) and maximum accumulation rate (V_{max}) values of the uptake kinetics were calculated after subtraction of the uptake at 4°C from that at 37°C and were determined by fitting the data to the Michaelis–Menten equation using nonlinear regression (GraphPad Prism, Graphpad Software, San Diego, CA, U.S.A.).

IC_{50} values were determined by nonlinear least square fitting of the data (one site competition), by the GraphPad Prism software.

Each graph point represents triplicate determinations, and results are based on at least three independent experiments.

Expression of FAAH

PC-3 cells were scrapped into 0.5 ml of ice-cold lysis buffer (50 mM Tris/HCl, pH 7.4; 5 mM ethylenediaminetetraacetic acid (EDTA); 1 mM ethylene glycol-bis (β-amino ethyl ether) tetraacetic acid (EGTA); 10 mM 2-mercaptoethanol containing 1 μg ml^{-1} leupeptin, 1 μg ml^{-1} aprotinin, 10 μg ml^{-1} soybean trypsin inhibitor and 1 mM PMSF). Cells were frozen, then thawed and subsequently disrupted by sonication after which they were centrifuged at 100,000 × g for 1 h. The pellet was resuspended in lysis buffer. Human prostate tissue specimens were obtained from 55- to 75-year-old patients undergoing open prostatectomy. The study protocol conformed to the Declaration of Helsinki, and was approved by the corresponding ethic committee. Prostate tissue was homogenized with a Polytron PT-20 tissue homogenizer (Kinematica, AG, Lucerne, Switzerland) at maximal speed in lysis buffer at 4°C. The homogenized tissue was filtered through a nylon mesh and centrifuged at 3500 × g for 5 min. The resulting supernatant was centrifuged at 30,000 × g for 20 min at 4°C. The pellet was washed in lysis buffer and centrifuged again at 30,000 × g for 20 min. The resulting pellet was homogenized and considered as membrane fraction. A similar protocol was followed for rat cerebellum tissue.

The amount of protein in each sample was determined using the protein assay kit (Bio-Rad, Richmond, CA, U.S.A.) and equivalent amounts (20 μg of protein) were analyzed by Western blot as previously described (Díaz-Laviada *et al*., 1990) using a primary polyclonal antibody against a peptide corresponding to residues 561–579 of the C-terminus of FAAH and previously characterized (Tsou *et al*., 1998). Blots were developed with the SuperSignal® chemiluminescent substrate from Pierce (Rockford, IL, U.S.A.).

Enzyme assay for FAAH and HPLC analysis

The assay of FAAH (EC 3.5.1.4) was performed by measuring the release of [^{3}H]AA from [^{3}H]ANA (see reagents for [^{3}H]ANA specification), using HPLC in cell extracts. PC-3 cells were washed in PBS, scraped in 50 mM Tris, pH 7.4, 1 mM EDTA and sonicated on ice with a microtip at maximum power three times for 10 s each in a cell disruptor Branson sonifier (American Laboratory Trading LLC). The homogenate was then centrifuged at 1000 × g for 10 min and the resulting pellet was diluted to a protein concentration of 1 mg ml^{-1}. For FAAH activity assay, several concentrations of anandamide in the presence or absence of 20 μM MAFP were added to a total volume of 200 μl hydrolase assay buffer (50 mM Tris-HCl, pH 9.0). The reaction was initiated by the addition of 20 μg of cellular extract and after incubation at 37°C for 20 min the reaction was stopped by the addition of 300 μl KOH (16%, v v^{-1}). The samples were treated sequentially with chloroform/methanol (2 : 1, v v^{-1}) and distilled water to obtain the lipidic and aqueous-soluble fractions as reported previously (Folch *et al*., 1957). The lipid extract was resuspended in methanol and used for anandamide and AA separation by HPLC. Separation was accomplished by reverse-phase HPLC with a Luna 5 μm-pore-size C_{18} column (250 nm × 4.60 mm; Phenomenex, Torrance, CA, U.S.A.). Anandamide and AA were eluted with acetonitrile/water (80 : 20, v v^{-1}) at a flow rate of 1.2 ml min^{-1}. The column effluent was monitored simultaneously by UV absorption spectroscopy (Beckman 168 variable-wavelength detector; Beckman Instruments, Palo Alto, CA, U.S.A.) and online radioactivity detection (using an LB-506 C-1 radioactivity detector; Berthold, Bad Widbad, Germany). Anandamide and AA were identified by comparison of the retention time of pure standards. FAAH activity was expressed as pmoles of arachidonate released per minute per milligram of protein.

Assay of affinity at cannabinoid receptors

Assay of affinity of UCM119 at cannabinoid receptors was carried out as previously described (López-Rodríguez *et al*., 2001b). Tissue and ligands, respectively, were for CB_1 receptor, rat cerebellar membranes and 0.5 nM [^{3}H]-WIN552122 and for CB_2 receptor, HEK293EBNA CB_2-transfected cell membranes and 0.3 nM [^{3}H]-CP55940 (for details, see López-Rodríguez *et al*., 2001b).

Results

Characterization of anandamide uptake by PC-3 cells

PC-3 cells were able to accumulate [^{3}H]-ANA, in a process which was temperature- (Figure 1a, only total and nonspecific ANA accumulation for one representative concentration is shown for the sake of clarity), concentration- (data not shown) and time-dependent and was saturable at 37°C (Figure 1b).

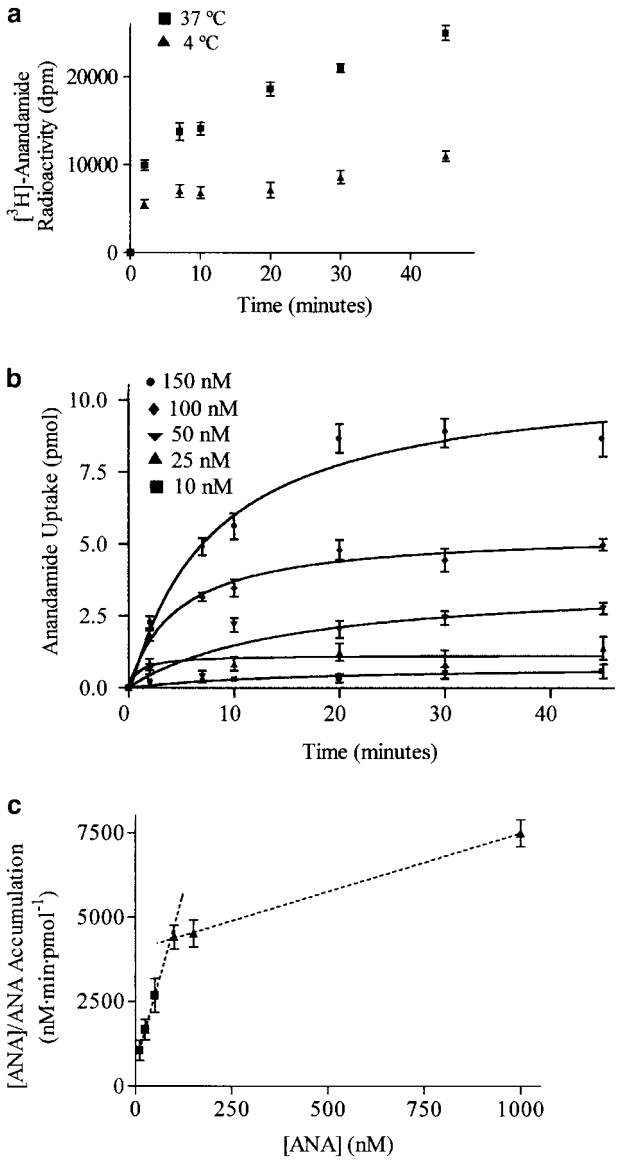

Figure 1 Temperature- and time-dependent accumulation of anandamide in PC-3 cells. (a) PC-3 cells were incubated with different concentrations of anandamide at either 37 or 4°C. Only total and nonspecific accumulation for one representative concentration of anandamide (150 nM) is shown for the sake of clarity. (b) PC-3 cells were incubated at 37°C with different concentrations of anandamide. Points represent specific anandamide accumulation at 37°C corrected for nonspecific binding at 4°C and are from one experiment representative of two independent assays performed in triplicate. The points were generated using GraphPad Prism and the curves were fitted using the one site binding hyperbola. (c) Hanes–Woolf analysis of anandamide accumulation under these conditions.

Kinetic analyses revealed that [^{3}H]-ANA uptake can be represented by two components of different affinities (Figure 1c). The higher affinity component ($K_M = 15.8$ nM, $V_{max} = 0.09$ pmol ANA min^{-1} (10^6 cells)$^{-1}$) may reflect very specific binding sites such as receptors, whereas the lower affinity component ($K_M = 1.2\,\mu$M, $V_{max} = 1.04$ pmol ANA min^{-1} (10^6 cells)$^{-1}$) is suggestive of a carrier-mediated transport as the apparent K_M value is similar to those of previously described anandamide transporters in other cells (Hillard & Jarrahian, 2000).

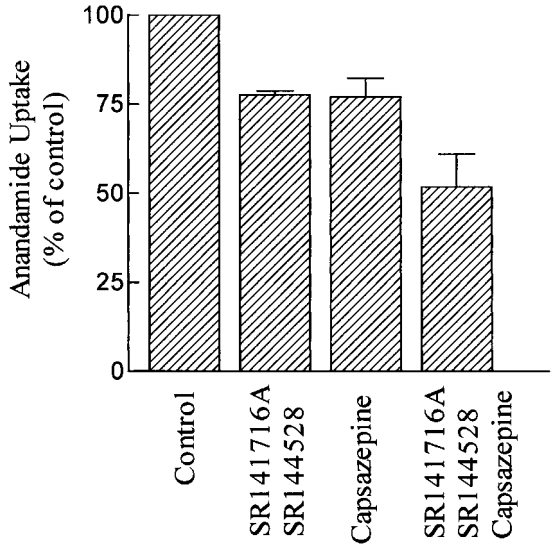

Figure 2 Effect of antagonists SR141716A, SR144528 and capsazepine on anandamide accumulation in PC-3 cells. PC-3 cells were preincubated at 37°C in the presence of the antagonists (50 μM) and incubated with 100 nM anandamide. The results represent specific anandamide accumulation at 37°C corrected for nonspecific binding at 4°C and are expressed as mean ± s.e. of two independent experiments performed in triplicate.

Influence of CB_1, CB_2 and VR_1 antagonists in the anandamide uptake

Due to the demonstrated presence of CB_1 and CB_2 cannabinoid receptors (Ruiz *et al*., 1999; Ruiz-Llorente *et al*., 2003) and to the potential existence of vanilloid receptor type 1 (VR_1) in PC-3 cells (unpublished results), and to displace the high-affinity component, we carried out an additional series of experiments aimed at determining the contribution of receptor binding in the quantification of anandamide incorporated into cells. The VR_1 antagonist capsazepine was able to displace anandamide uptake in a dose-dependent manner, with 50 μM being the most effective concentration inferred from its dose–inhibition curve (data not shown). Anandamide uptake was then measured in the presence of the vanilloid antagonist capsazepine (50 μM), cannabinoid CB_1 antagonist SR141716A (50 μM) and cannabinoid CB_2 antagonist SR144528 (50 μM). The three antagonists, when incubated together, were able to displace about 40% of the total specific bound [^{3}H]-ANA (Figure 2); so in order to avoid this receptor-bound contribution, all the experiments were performed in the presence of 50 μM of the antagonists. Anandamide accumulation, measured under these conditions, was time-, concentration- and temperature-dependent (Figure 3a–c). Kinetic studies of anandamide uptake, determined under these conditions (Figure 3d), fitted to one straight line, which revealed apparent parameters of $K_M = 4.9 \pm 0.2\,\mu$M and $V_{max} = 3.3 \pm 0.3$ pmol min^{-1} (10^6 cells)$^{-1}$.

Expression and activity of FAAH in prostate PC-3 cells

Considering that diverse studies (Deutsch *et al*., 2001; Patricelli & Cravatt, 2001; Hillard & Jarrahian, 2003) suggest the existence of crossregulation between the FAAH and the

anandamide transporter, we analyzed the expression of FAAH by prostate cells. Both epithelial prostate cells and human prostate tissue express FAAH protein, as detected by Western blot (Figure 4). FAAH polyclonal antibodies, previously validated by antigen competition experiments (Tsou *et al*., 1998), recognized two bands in human prostate tissue. The major band corresponds to a molecular mass of 69 kDa, which is a little higher than the predicted molecular mass for the human FAAH (Giang & Cravatt, 1997) but is similar to the FAAH band observed in mouse uterus (Maccarrone *et al*., 2000b) and to the band detected in rat cerebellum, used as positive control (Figure 4). The minor band of 73.2 kDa was also detected in the prostate cell lines PC-3 and LNCaP (Figure 4) and could correspond to different isoforms.

To further investigate the activity of the FAAH expressed in prostate PC-3 cells, we measured the released [^{3}H]AA from [^{3}H]ANA in cell extracts by HPLC. Sharp and well-resolved ANA and AA peaks were obtained (Figure 5a). FAAH activity, expressed as pmoles of AA released per minute per milligram of protein, was concentration-dependent and saturable (Figure 5b). FAAH activity detected in PC-3 cells was almost completely inhibited by 20 μM MAFP (Figure 5b), a potent and selective inhibitor of FAAH (Deutsch *et al*., 1997), reinforcing the notion that FAAH is expressed in prostate PC-3 cells.

Evaluation of the influence of FAAH or other lipid transporters in anandamide uptake

Since PC-3 cells express FAAH, we next tested the influence of the FAAH inhibitors MAFP and PMSF on anandamide

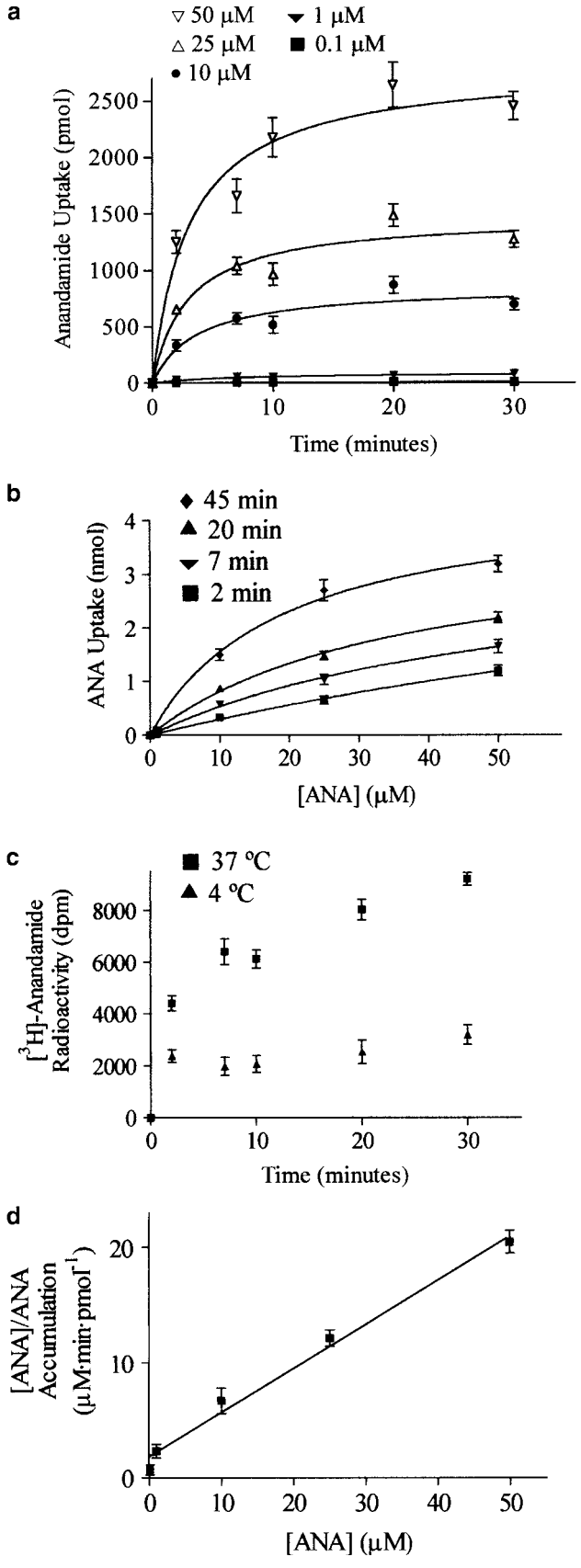

Figure 3 Time, concentration and temperature dependence of anandamide uptake in PC-3 cells. (a) PC-3 cells were preincubated at 37°C in the presence of SR141716A, SR144528 and capsazepine (50 μM), and incubated with different concentrations of anandamide. (b) PC-3 cells were preincubated at 37°C in the presence of SR141716A, SR144528 and capsazepine (50 μM), and incubated for different times. The results represent specific anandamide accumulation at 37°C corrected for nonspecific binding at 4°C and are expressed as mean ± s.e. of two independent experiments performed in triplicate. The points were generated using GraphPad Prism, and the curves were fitted using the one site binding hyperbola. (c) PC-3 cells were incubated with different concentrations of anandamide at either 37 or 4°C. Only total and nonspecific accumulation for one representative concentration of anandamide (1 μM) is shown for the sake of clarity. (d) Hanes–Woolf analysis of anandamide accumulation under these conditions.

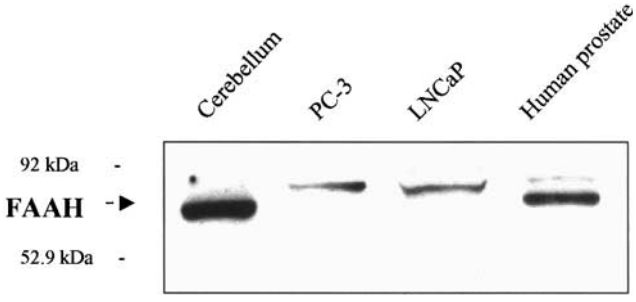

Figure 4 Expression of FAAH enzyme in prostate epithelial cells and human prostate gland. Particulate fraction of the prostate cellular lines PC-3 and LNCaP as well as human prostate tissue (HP) and rat cerebellum (C) used as positive control were resolved by electrophoresis, transferred and then incubated with a polyclonal specific antibody anti-FAAH. Molecular weight markers are shown on the left.

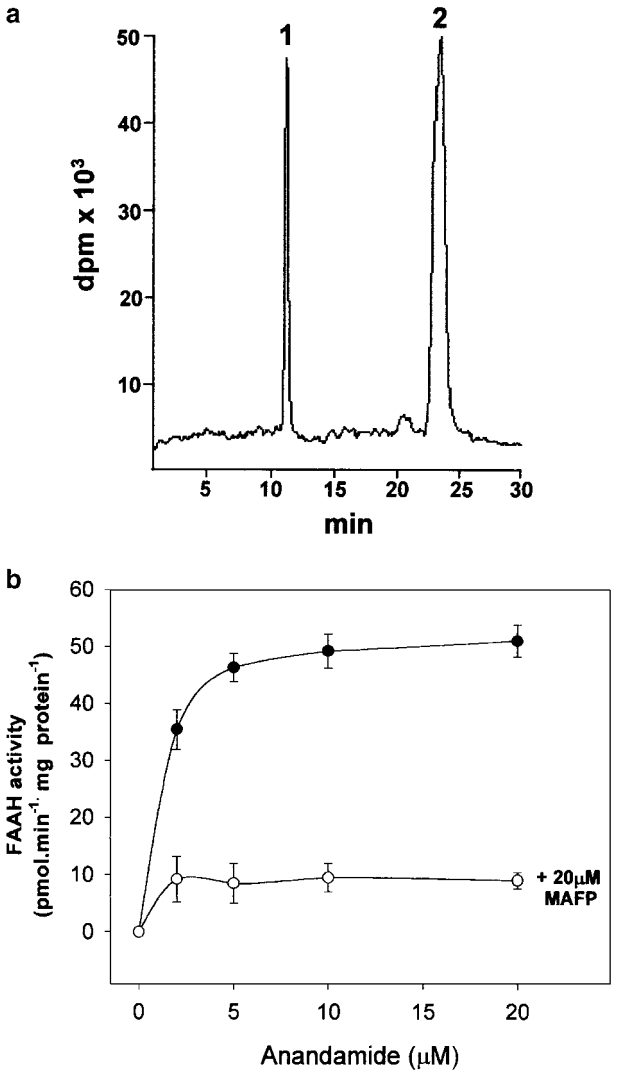

Figure 5 FAAH activity in PC-3 cells. (a) Resolved peaks of ANA (1) and AA (2) by HPLC. (b) FAAH activity was measured at pH 9.0 and 37°C in cellular extracts incubated with increasing [^{3}H]ANA ± 20 μM MAFP. The released [^{3}H]AA was measured using HPLC as described in the Methods section.

transport, in order to assess whether anandamide hydrolysis was affecting the uptake process. In these experiments, PMSF, tested at a concentration of 100 μM, was not able to induce significant inhibition (less than 9%) in the anandamide uptake process whereas MAFP inhibited anandamide incorporation into cells by 30% (Figure 6).

Additionally, and in order to rule out the involvement of other lipid transporters previously described, we examined the effect of several nonselective transport inhibitors on the accumulation of anandamide such as verapamil or phloretin at concentrations previously used to characterize other anandamide uptake processes (Beltramo *et al*., 1997; Hillard *et al*., 1997). Neither verapamil (100 μM), which behaves as a phospholipid uptake inhibitor (Beltramo *et al*., 1997), nor phloretin (100 μM), which has been characterized as an inhibitor of diverse carrier-mediated uptake processes including the accumulation of fatty acids by adipocytes and glucose and anion transport into erythrocytes (Hillard *et al*., 1997),

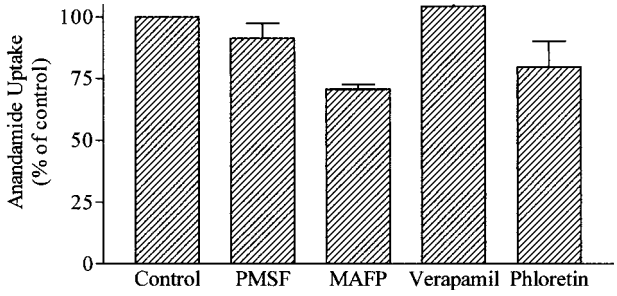

Figure 6 Effect of FAAH inhibitors and lipid transport inhibitors phloretin and verapamil on anandamide uptake in PC-3 cells. PC-3 cells were preincubated at 37°C in the presence of SR141716A, SR144528 and capsazepine (50 μM), and incubated with 100 nM anandamide in the presence of the corresponding FAAH or lipid transport inhibitor (100 μM). The results represent specific anandamide accumulation at 37°C corrected for nonspecific binding at 4°C and are expressed as mean ± s.e. of two independent experiments performed in duplicate.

was able to exert any appreciable capacity to inhibit anandamide transport (Figure 6), with inhibition values not significantly different from control, of about 0 and 20%, respectively.

Synthesis of new anandamide uptake inhibitors

As the following step in the search of more potent anandamide transport inhibitors in order to get deeper insights into the structural requirements involved in the recognition of compounds for this carrier, we synthesized a series of structurally different analogs (**1**–**8**) and evaluated their capacity as transporter inhibitors. Compounds **1**–**8** (Figure 7) were synthesized following the methods detailed in the Methods section.

Inhibition of the anandamide uptake

The newly synthesized compounds (tested at 100 μM as the maximal concentration) showed different efficacy as uptake inhibitors, ranging from negligible capacity of compound **3** to 49% of inhibition produced by compound **4**, which was comparable to the inhibition produced by the transporter selective inhibitor VDM11 (Figure 8). [^{3}H]ANA uptake was moderately inhibited in a dose-dependent manner by the endocannabinoid transporter inhibitor AM404 (Figure 9). However, the maximal concentration used, 100 μM, which was previously shown to cause 70% inhibition in neurons and astrocytes (Beltramo *et al*., 1997), only reduced the transport to about a 25% of the untreated control (Figure 9). Compound **4** (UCM119) exhibits an IC_{50} value of 11.3 μM as shown from its dose–response curve (Figure 9) and was as potent as VDM11 (IC_{50} value of 10.89 μM) in PC-3 prostate cells (Figure 9).

Additionally, and to study the selectivity degree of this compound, we carried out binding assays to determine the affinity for both cannabinoid receptors. Compound **4** shows little affinity for both cannabinoid receptors (K_i (CB_1) > 5000 nM; K_i (CB_2) > 1000 nM) especially if we compare

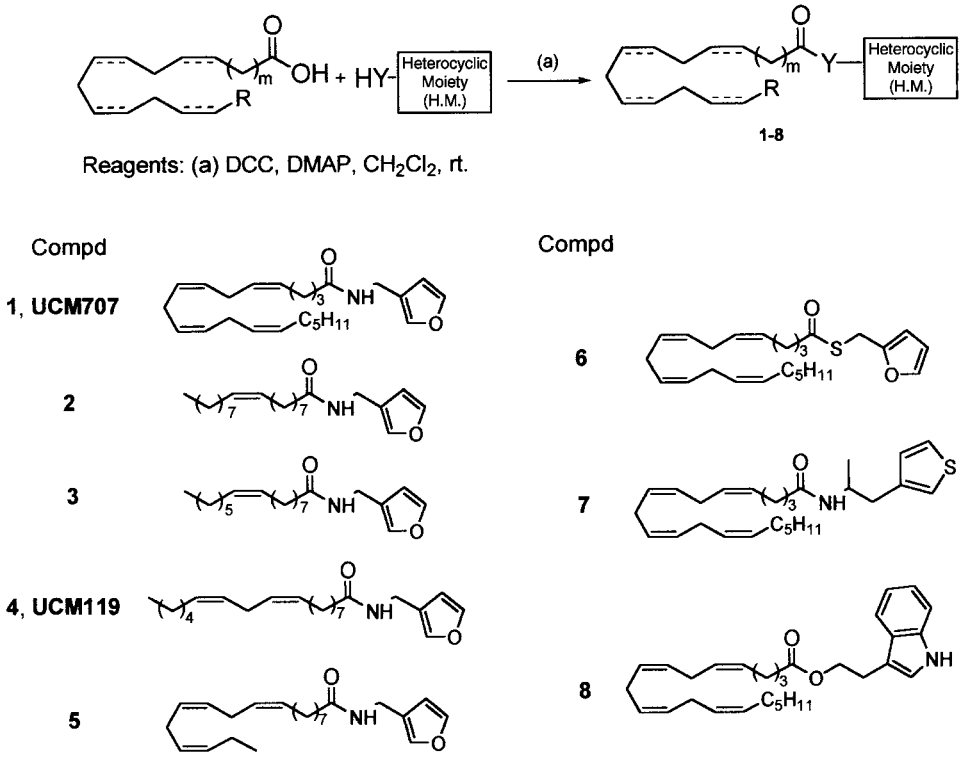

Figure 7 Chemical structures of synthesized anandamide uptake inhibitors (**1**–**8**). Compounds **1**–**8** were synthesized according to the procedure detailed in the Methods section.

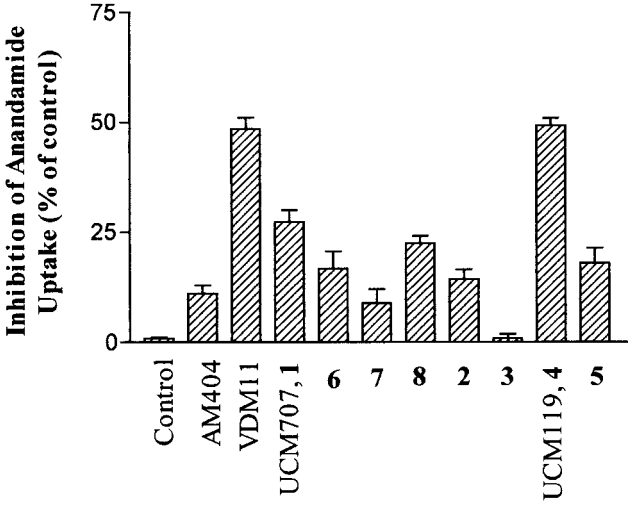

Figure 8 Inhibition of anandamide uptake of compounds **1**–**8** in PC-3 cells. PC-3 cells were preincubated at 37°C in the presence of SR141716A, SR144528 and capsazepine (50 μM), and incubated with 100 nM anandamide in the presence of AM404, VDM11 or the corresponding compound **1**–**8** (100 μM). The results represent specific anandamide accumulation at 37°C corrected for nonspecific binding at 4°C and are expressed as mean ± s.e. of two independent experiments performed in duplicate.

these values with those obtained for other cannabinoid ligands such as WIN552122 or CP55940 with K_i values in the low nanomolar range (López-Rodríguez *et al*., 2001b).

Discussion

The objective of these studies was to demonstrate the existence of an inactivation system for anandamide, including a carrier-mediated process responsible for anandamide uptake as well as the expression of FAAH, and to characterize this putative transporter in epithelial PC-3 cells.

The accumulation of exogenous [^{3}H]-ANA by these cells fulfills the main features of a carrier-mediated transport. It is temperature-, concentration- and time-dependent, showing a $t_{1/2}$ value of about 5 min. The K_M and V_{max} values obtained from the kinetic studies revealed similar maximal accumulation rates and affinity values of this transporter compared with other studies previously reported examining anandamide uptake in both peripheral and central nervous system-derived cells (for a review, see López-Rodríguez *et al*., 2002).

Kinetic assays carried out in the presence of CB_1, CB_2 and VR_1 receptor antagonists revealed K_M and V_{max} values of 4.9 μM and 3.3 pmol min^{-1} (10^6 cells)$^{-1}$. As expected, the kinetic analysis fitted a straight line, which reflects exclusively the interaction with the transporter, once the receptor influence is eliminated. This K_M value, in the low micromolar range, is very similar to those obtained for other neurotransmitter uptake systems (Beltramo *et al*., 1997).

In order to consider only the transporter component, we carried out the rest of the experiments coincubating with these three antagonists. However, and even under these conditions, neither AM404 nor UCM707 was able to induce any remarkable inhibitory effects. However, this is not a surprising finding since important differences among different cells have

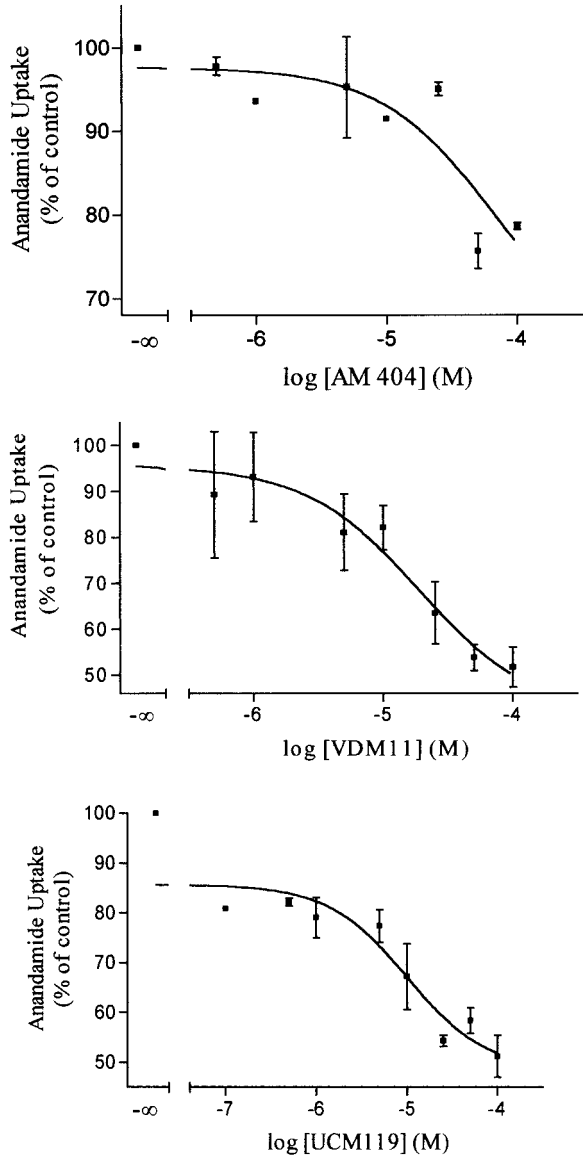

Figure 9 Inhibition of anandamide accumulation by AM404, VDM11 and UCM119 (compound **4**) in PC-3 cells. PC-3 cells were preincubated at 37°C in the presence of SR141716A, SR144528 and capsazepine (50 μM), and incubated with 100 nM anandamide in the presence of diverse concentrations of AM404, VDM11 or UCM119 (compound **4**). The results represent specific anandamide accumulation at 37°C corrected for nonspecific binding at 4°C and are expressed as mean ± s.e. of two independent experiments performed in duplicate. The points were generated using GraphPad Prism, and the curves were obtained using the sigmoidal dose–response fit.

been reported regarding different sensitivities toward chemicals such as NO or alkylating agents, the proper AM404 or even the endocannabinoids (for a review, see López-Rodríguez *et al*., 2002). Our results are similar to those obtained in platelets in which an insensitivity to AM404 inhibition was also observed (Maccarrone *et al*., 2001).

Prostate PC-3 cells as well as human prostate tissue express FAAH enzyme corroborated by Western blot and activity assay. FAAH antibodies recognized two bands of 69 and 73.2 kDa, whereas mainly the upper band was detected in prostate cells. Data from our laboratory reveal that there is differential expression of this two bands among different patients (unpublished results). As FAAH expression is steroid-regulated (Maccarrone *et al*., 2000b; Waleh *et al*., 2002), the expression of the upper band in prostate cell lines could be due to the particular hormone situation of these cells. FAAH expressed in PC-3 cells was active and was inhibited by the potent FAAH inhibitor MAFP. The results demonstrate the existence of an anandamide degradation system in PC-3 cells.

There exists a recent controversy about the existence of a specific anandamide transporter suggesting that intracellular anandamide hydrolysis by FAAH may be responsible for the observed saturations of anandamide incorporation into cells (Glaser *et al*., 2003; Hillard & Jarrahian, 2003). In a first attempt to examine the influence of FAAH as well as other lipid transporters, we determined the ability of PMSF and MAFP to inhibit the anandamide uptake. Only MAFP produced a 30% inhibition of the incorporation process, suggesting that anandamide hydrolysis may participate in the anandamide uptake process but it is not responsible for all the accumulated anandamide. The FAAH inhibitor MAFP has been used in previous studies to examine the role of FAAH activity in the transport of anandamide (Day *et al*., 2001; Deutsch *et al*., 2001; Glaser *et al*., 2003). However, in these studies, a 50–90% of transport inhibition was obtained. Moreover, in cells lacking FAAH, MAFP but not PMSF reduced anandamide transport (Day *et al*., 2001) suggesting that another mechanism different from FAAH exists and it may be inhibited by MAFP (Day *et al*., 2001). On the other hand, PMSF only inhibited anandamide transport in FAAH expressing cells, suggesting that the inhibition detected with PMSF is due to the FAAH component. In our studies, PMSF did not cause transport inhibition, supporting the notion that other components besides FAAH participate in the process of anandamide accumulation. Another recent study shows that in rabbit platelets, which do not possess a carrier-mediated mechanism for anandamide but express an active FAAH, MAFP did not affect anandamide uptake although it inhibited anandamide degradation (Fasia *et al*., 2003).

We tested nonselective inhibitors of other lipid transporter systems like verapamil and phloretin, and neither of these agents appreciably inhibited anandamide transport, a fact that indicates the existence in PC-3 cells of an anandamide uptake system different from other lipid transporter proteins.

To search for more potent anandamide transport inhibitors in PC-3 cells, we synthesized and tested a series of structural analogs of anandamide (compounds **1**–**8**) and compared them with previously characterized inhibitors like AM404, VDM11 and UCM707, which have allowed us to set up a structure–activity relationship (SAR) study focused on determining the main structural features involved in the interaction of compounds with the putative anandamide transporter characterized in PC-3 cells.

In these derivatives, we have carried out structural modifications in different parts of anandamide including changes in the fatty acid chain as well as the substitution of its ethanolamine moiety for a heterocycle (Figure 7). Thus, as a first approach, we have modified the heterocyclic moiety, the length and branching between the AA chain and the heterocycle, and we have also replaced the amide moiety for ester or thioester groups (compounds **1, 6**–**8**). Among these AA derivatives, the fur-3-ylmethylamine moiety together with an amide group exhibits the major inhibitory potency. As

representative examples, Figure 8 shows the inhibitory values obtained for compounds **6**, **7** and **8** vs **1** (16.8, 9 and 22.4 vs 25%, respectively).

In order to evaluate the influence of the fatty acid chain in the interaction with the transporter, we replaced the AA moiety with different fatty acid chains bearing distinct chain lengths (16 and 18 carbon atoms) and diverse number of insaturations (compounds **1–5**).

Regarding the number of insaturations, the presence of two double bonds enhances the affinity for the transporter, as deduced from the inhibition value obtained for compound **4**, the most potent derivative of this series of compounds, which was able to inhibit nearly half of anandamide transport (49%).

Increasing or decreasing the number of double bonds implied in all cases important reductions in the inhibitory ability. For instance, compound **2**, with one double bond, and compound **5**, with three double bonds, exhibit comparable inhibition values (15.8 and 18.1%, respectively). These results point to the existence of an optimum folded conformation that depends on the number of insaturations.

Additionally, compound **3** allowed us to evaluate the effect of reducing the hydrophobic length chain. The fact that this compound is not able to inhibit the transporter reflects the ability of the carrier to distinguish between structural analogs.

Although previous SAR studies have identified a series of more potent anandamide uptake inhibitors in other cell types such as astrocytoma, neurons or lymphoma cells (Piomelli *et al*., 1999; Jarrahian *et al*., 2000; López-Rodríguez *et al*., 2003), the series of analogs reported here is the first one that has been analyzed in PC-3 prostate cells. Moreover, the partial efficacy that all of these inhibitors (**1**–**8**) and previously characterized inhibitors (AM404 and VDM11) display to inhibit the anandamide uptake in PC-3 cells even at the highest doses used reveals the lack of an optimal molecular interaction between the putative carrier and the synthesized analogs. Further structural optimization of compounds is still required in order to develop inhibitors that are able to block completely the anandamide uptake process in PC-3 cells.

In this context, these new synthesized inhibitors, especially UCM119, suppose a starting point in the development of new tools for the study of other anandamide transport systems in which AM404 or other classical transporter inhibitors are not effective.

Taken together, the above data show the existence of recognition selectivity among analogs with similar chemical structures, one of the most important features exhibited by protein-mediated processes, thus giving further support to the existence of a facilitated uptake phenomenon responsible for anandamide transport in PC-3 cells. Undoubtedly, more detailed studies will be necessary to further characterize the transporter and to establish the involvement and importance of this process both physiologically and therapeutically, especially with regard to their potential utility for the management of tumoral processes in which this cell line is implicated (Ruiz *et al*., 1999).

In conclusion, the results reported here demonstrate that prostate cells incorporate anandamide in a process kinetically comparable to that described in other cells. The transport process is different from other lipid transporters, since it is not affected by inhibitors of other lipid carriers. Moreover, the minor effect observed after incubation in the presence of PMSF and MAFP seems to indicate that anandamide hydrolysis is not the only driving force for anandamide transport into PC-3 cells, at least within the time frame of our experiments.

The identification of anandamide carrier-mediated transport together with the expression of FAAH in PC-3 cells represents the first characterization of an anandamide degradation system in prostate cells and reinforces the role of endocannabinoids as neuroendocrine regulators.

This investigation was supported by Ministerio de Ciencia y Tecnología (BQU 2001-1459 and SAF 2002-01572) and by Agencia Antidroga de la Comunidad de Madrid. L. Ruiz-Llorente and S. Ortega-Gutiérrez are fellows from the Ministerio de Educación, Cultura y Deporte and M.G. Sánchez is fellow from Universidad de Alcalá. We thank *Unidad de Cultivos* from Universidad de Alcalá for technical assistance and Sanofi Recherche for SR141716A and SR144528 gift.

References

AHLUWALIA, B.S., RAJGURU, S.U. & NOLAN, G.H. (1985). The effect of Δ9-tetrahydrocannabinol *in utero* exposure on rat offspring fertility and ventral prostate gland morphology. *J. Androl.,* **6,** 386–391.

AMERI, A. (1999). The effects of cannabinoids on the brain. *Prog. Neurobiol.,* **58,** 315–348.

BELTRAMO, M., STELLA, N., CALIGNANO, A., LIN, S.Y., MAKRIYANNIS, A. & PIOMELLI, D. (1997). Functional role of high-affinity anandamide transport, as revealed by selective inhibition. *Science,* **277,** 1094–1097.

BISOGNO, T., MAURELLI, S., MELCK, D., DE PETROCELLIS, L. & DI MARZO, V. (1997). Biosynthesis, uptake and degradation of anandamide and palmitoylethanolamide in leukocytes. *J. Biol. Chem.,* **272,** 3315–3323.

CRAVATT, B.F. & LICHTMAN, A.H. (2003). Fatty acid amide hydrolase: an emerging therapeutic target in the endocannabinoid system. *Curr. Opin. Chem. Biol.,* **7,** 469–475.

DAY, T.A., RAKHSHAN, F., DEUTSCH, D.G. & BARKER, E.L. (2001). Role of fatty acid amide hydrolase in the transport of the endogenous cannabinoid anandamide. *Mol. Pharmacol.,* **59,** 1369–1375.

DEUTSCH, D.G., GLASER, S.T., HOWELL, J.M., KUNZ, J.S., PUFFENBARGER, R.A., HILLARD, C.J. & ABUMRAD, N. (2001). The cellular uptake of anandamide is coupled to its breakdown by fatty-acid amide hydrolase. *J. Biol. Chem.,* **276,** 6967–6973.

DEUTSCH, D.G., OMEIR, R., ARREAZA, G., SALEHANI, D., PRESTWICH, G.D., HUANG, Z. & HOWLETT, A. (1997). Methyl arachidonyl fluorophosphonate: a potent irreversible inhibitor of anandamide amidase. *Biochem. Pharmacol.,* **53,** 255–260.

DEUTSCH, D.G., UEDA, N. & YAMAMOTO, S. (2002). The fatty acid amide hydrolase (FAAH). *Prostaglandins Leukot. Essent. Fatty Acids,* **66,** 201–210.

DEVANE, W.A., HANUS, L., BREUER, A., PERTWEE, R.G., STEVENSON, L.A., GRIFFIN, G., GIBSON, D., MANDELBAUM, A., ETINGER, A. & MECHOULAM, R. (1992). Isolation and structure of a brain constituent that binds to the cannabinoid receptor. *Science,* **258,** 1946–1949.

DÍAZ-LAVIADA, I., LARRODERA, P., DÍAZ-MECO, M.T., CORNET, M.E., GUDDAL, P.H., JOHANSEN, T. & MOSCAT, J. (1990). Evidence for a role of phosphatidylcholine-hydrolysing phospholipase C in the regulation of protein kinase C by ras and src oncogenes. *EMBO J.,* **9,** 3907–3912.

DI MARZO, V., FONTANA, A., CADAS, H., SCHINELLI, S., SCHWARTZ, J.C. & PIOMELLI, D. (1994). Formation and inactivation of endogenous cannabinoid anandamide in central neurons. *Nature,* **372,** 686–691.

DI MARZO, V., MELCK, D., BISOGNO, T. & DE PETROCELLIS, L. (1998). Endocannabinoids: endogenous cannabinoid receptor ligands with neuromodulatory action. *Trends Neurosci.,* **21,** 521–528.

FASIA, L., KARAVA, V. & SIAFAKA-KAPADAI, A. (2003). Uptake and metabolism of [^{3}H]anandamide by rabbit platelets. *Eur. J. Biochem.,* **270,** 3498–3506.

FOLCH, J., LEES, M. & SLOANE STANLEY, G.H. (1957). A simple method for the isolation and purification of total lipids from animal tissue. *J. Biol. Chem.,* **226,** 497–509.

FOWLER, C.J. & JACOBSSON, S.O. (2002). Cellular transport of anandamide, 2-arachidonoylglycerol and palmitoylethanolamide-targets for drug development? *Prostaglandins Leukot. Essent. Fatty Acids,* **66,** 193–200.

FOWLER, C.J., TIGER, G., LÓPEZ-RODRÍGUEZ, M.L., VISO, A., ORTEGA-GUTIÉRREZ, S. & RAMOS, J.A. (2003). Inhibition of fatty acid amidohydrolase, the enzyme responsible for the metabolism of the endocannabinoid anandamide, by analogues of arachidonoyl-serotonin. *J. Enzyme Inhib. Med. Chem.,* **18,** 225–231.

GIANG, D.K. & CRAVATT, B.F. (1997). Molecular characterization of human and mouse fatty acid amide hydrolases. *Proc. Natl. Acad. Sci. U.S.A.,* **94,** 2238–2242.

GIUFFRIDA, A., BELTRAMO, M. & PIOMELLI, D. (2001). Mechanisms of endocannabinoid inactivation: biochemistry and pharmacology. *J. Pharmacol. Exp. Ther.,* **298,** 7–14.

GLASER, S.T., ABUMRAD, N.A., FATADE, F., KACZOCHA, M., STUDHOLME, K.M. & DEUTSCH, D.G. (2003). Evidence against the presence of an anandamide transporter. *Proc. Natl. Acad. Sci. U.S.A.,* **100,** 4269–4274.

HARCLERODE, J. (1984). Endocrine effects of marijuana in the male: preclinical studies. *NIDA Res. Monogr.,* **44,** 46–64.

HILLARD, C.J., EDGEMOND, W.S., JARRAHIAN, A. & CAMPBELL, W.B. (1997). Accumulation of *N*-arachidonoylethanolamine (anandamide) into cerebellar granule cells occurs *via* facilitated diffusion. *J. Neurochem.,* **69,** 631–638.

HILLARD, C.J. & JARRAHIAN, A. (2000). The movement of *N*-arachidonoylethanolamine (anandamide) across cellular membranes. *Chem. Phys. Lipids,* **108,** 123–134.

HILLARD, C.J. & JARRAHIAN, A. (2003). Cellular accumulation of anandamide: consensus and controversy. *Br. J. Pharmacol.,* **140,** 802–808.

JARRAHIAN, A., MANNA, S., EDGEMOND, W.S., CAMPBELL, W.B. & HILLARD, C.J. (2000). Structure–activity relationships among *N*-arachidonylethanolamine (anandamide) head group analogues for the anandamide transporter. *J. Neurochem.,* **74,** 2597–2606.

KLEIN, T.W., NEWTON, C.A. & FRIEDMAN, H. (2001). Cannabinoids and the immune system. *Pain Res. Manage.,* **6,** 95–101.

LÓPEZ-RODRÍGUEZ, M.L., VISO, A., ORTEGA-GUTIÉRREZ, S., FERNÁNDEZ-RUIZ, J. & RAMOS, J.A. (2002). Endocannabinoid transporter inhibitors. *Curr. Med. Chem. Central Nervous System Agents,* **2,** 129–141.

LÓPEZ-RODRÍGUEZ, M.L., VISO, A., ORTEGA-GUTIÉRREZ, S., FOWLER, C.J., TIGER, G., DE LAGO, E., FERNÁNDEZ-RUIZ, J. & RAMOS, J.A. (2003). Design, synthesis and biological evaluation of new endocannabinoid uptake process inhibitors: comparison with effects upon fatty acid amidohydrolase. *J. Med. Chem.,* **46,** 1512–1522.

LÓPEZ-RODRÍGUEZ, M.L., VISO, A., ORTEGA-GUTIÉRREZ, S., LASTRES-BECKER, I., GONZÁLEZ, S., FERNÁNDEZ-RUIZ, J. & RAMOS, J.A. (2001a). PCT/ES01/00305 (WO 02/12167 A1).

LÓPEZ-RODRÍGUEZ, M.L., VISO, A., ORTEGA-GUTIÉRREZ, S., LASTRES-BECKER, I., GONZÁLEZ, S., FERNÁNDEZ-RUIZ, J. & RAMOS, J.A. (2001b). Design, synthesis and biological evaluation of novel arachidonic acid derivatives as highly potent and selective endocannabinoid transporter inhibitors. *J. Med. Chem.,* **44,** 4505–4508.

MACCARRONE, M., BARI, M., BATTISTA, N. & FINAZZI-AGRÒ, A. (2002). Estrogen estimulates arachidonoylethanolamide release from human endothelial cells and platelet activation. *Blood,* **100,** 4040–4048.

MACCARRONE, M., BARI, M., LORENZON, T., BISOGNO, T., DI MARZO, V. & FINAZZI-AGRÒ, A. (2000a). Anandamide uptake by human endothelial cells and its regulation by nitric oxide. *J. Biol. Chem.,* **275,** 13484–13492.

MACCARRONE, M., BARI, M., MENICHELLI, A., GIULIANI, E., DEL PRINCIPE, D. & FINAZZI-AGRO, A. (2001). Human platelets bind and degrade 2-arachidonoylglycerol, which activates these cells through a cannabinoid receptor. *Eur. J. Biochem.,* **268,** 819–825.

MACCARRONE, M., CECCONI, S., ROSSI, G., BATTISTA, N., PAUSELLI, R. & FINAZZI-AGRÒ, A. (2003). Anandamide activity and degradation are regulated by early postnatal aging and follicle-stimulating hormone in mouse sertoli cells. *Endocrinology,* **144,** 20–28.

MACCARRONE, M., DE FELICI, M., BARI, M., KLINGER, F., SIRACUSA, G. & FINAZZI-AGRO, A. (2000b). Down-regulation of anandamide hydrolase in mouse uterus by sex hormones. *Eur. J. Biochem.,* **267,** 2991–2997.

MELCK, D., DE PETROCELLIS, L., ORLANDO, P., BISOGNO, T., LAEZZA, C., BIFULCO, M. & DI MARZO, V. (2000). Supression of nerve growth factor Trk receptors and prolactin receptors by endocannabinoids leads to inhibition of human breast and prostate cancer cell proliferation. *Endocrinology,* **141,** 118–126.

MIMEAULT, M., POMMERY, N., WATTEZ, N., BAILLY, C. & HENICHART, J. (2003). Anti-proliferative and apoptotic effects of anandamide in human prostatic cencer cell lines: implication of epidermal growth factor receptor down-regulation and ceramide production. *Prostate,* **56,** 1–12.

PATRICELLI, M.P. & CRAVATT, B.F. (2001). Proteins regulating the biosynthesis and inactivation of neuromodulatory fatty acid amides. *Vitam. Horm.,* **62,** 95–131.

PIOMELLI, D., BELTRAMO, M., GLASNAPP, S., LIN, S.Y., GOUTOPOULOS, A., XIE, X.-Q. & MAKRIYANNIS, A. (1999). Structural determinants for recognition and translocation by the anandamide transporter. *Proc. Natl. Acad. Sci. U.S.A.,* **96,** 5802–5807.

PUROHIT, V., AHLUWAHLIA, B.S. & VIGERSKY, R.A. (1980). Marihuana inhibits dihydrotestosterone binding to the androgen receptor. *Endocrinology,* **107,** 848–850.

RUIZ, L., MIGUEL, A. & DÍAZ-LAVIADA, I. (1999). 9-Tetrahydrocannabinol induces apoptosis in human prostate PC-3 cells *via* a receptor-independent mechanism. *FEBS Lett.,* **458,** 400–404.

RUIZ-LLORENTE, L., SÁNCHEZ, M.G., CARMENA, M.J., PRIETO, J.C., SÁNCHEZ-CHAPADO, M., IZQUIERDO, A. & DÍAZ-LAVIADA, I. (2003). Expression of functionally active cannabinoid receptor CB_1 in the human prostate gland. *Prostate,* **54,** 95–102.

SÁNCHEZ, M.G., RUIZ-LLORENTE, L., SÁNCHEZ, A.M. & DÍAZ-LAVIADA, I. (2003). Activation of phosphoinositide 3-kinase/PKB pathway by CB_1 and CB_2 cannabinoid receptors expressed in prostate PC-3 cells. Involvement in Raf-1 stimulation and NGF induction. *Cell Signal,* **15,** 851–859.

SCHUEL, H., BURKMAN, L.J., LIPPES, J., CRICKARD, K., FORESTER, E., PIOMELLI, D. & GIUFFRIDA, A. (2002). *N*-acylethanolamines in human reproductive fluids. *Chem. Phys. Lipids,* **121,** 211–227.

SMART, D., GUNTHORPE, M.J., JERMAN, J.C., NASIR, S., GRAY, J., MUIR, A.I., CHAMBERS, J.K., RANDALL, A.D. & DAVIS, J.B. (2000). The endogenous lipid anandamide is a full agonist at the human vanilloid receptor (hVR_1). *Br. J. Pharmacol.,* **129,** 227–230.

SUGIURA, T. & WAKU, K. (2002). Cannabinoid receptors and their endogenous ligands. *J. Biochem.,* **132,** 7–12.

TSOU, K., NOGUERON, M.I., MUTHIAN, S., SAÑUDO-PEÑA, M.C., HILLARD, C.J., DEUTSCH, D.G. & WALKER, J.M. (1998). Fatty acid amide hydrolase is located preferentially in large neurons in the rat central nervous system as revealed by immunohistochemistry. *Neurosci. Lett.,* **254,** 137–140.

VELASCO, L., RUIZ, L., SÁNCHEZ, M.G. & DÍAZ-LAVIADA, I. (2001). 9-Tetrahydrocannabinol increases nerve growth factor production by prostate PC-3 cells. *Eur. J. Biochem.,* **268,** 531–535.

WALEH, N.S., CRAVATT, B.F., APTE-DESHPANDE, A., TERAO, A. & KILDUFF, T.S. (2002). Transcriptional regulation of the mouse fatty acid amide hydrolase gene. *Gene,* **291,** 203–210.

WENGER, T., LEDENT, C., CSERNUS, V. & GERENDAI, I. (2001). The central cannabinoid receptor inactivation suppresses endocrine reproductive functions. *Biochem. Biophys. Res. Commun.,* **284,** 363–368.

WENGER, T. & MOLDRICH, G. (2002). The role of endocannabinoids in the hypothalamic regulation of visceral functions. *Prostaglandins Leukot. Essent. Fatty Acids,* **66,** 301–307.

WILSON, R.I. & NICOLL, R.A. (2002). Endocannabinoid signaling in the brain. *Science,* **296,** 678–682.

(Received September 21, 2003
Revised October 15, 2003
Accepted November 11, 2003)